

The open LPC Paul trap for precision measurements in beta decay

P. Delahaye^{1,2}, G. Ban², M. Benali², D. Durand², X. Fabian³, X. Fléhard², M. Herbane², E. Liénard², F. Mauger², A. Méry⁴, Y. Merrer², O. Naviliat-Cuncic^{2,5}, G. Quémener², B. M. Retailleau¹, D. Rodriguez⁶, J. C. Thomas¹, P. Ujic¹

¹GANIL, CEA/DSM-CNRS/IN2P3, Bd Henri Becquerel, 14000 Caen, France

²Normandie Univ, ENSICAEN, UNICAEN, CNRS/IN2P3, LPC Caen, 14000 Caen, France

³Institut de Physique nucléaire de Lyon, 4 rue Enrico Fermi, 69622 Villeurbanne, France

⁴CIMAP, CEA/CNRS/ENSICAEN, Université de Caen, Caen, France

⁵Departamento de Física Atómica Molecular y Nuclear, Universidad de Granada, Granada, Spain

⁶National Superconducting Cyclotron Laboratory and Department of Physics and Astronomy, Michigan State University, East Lansing MI 48824, USA

Corresponding author : delahaye@ganil.fr

Abstract. The LPCTrap experiment uses an open Paul trap which was built to enable precision measurements in the beta decay of radioactive ions. The initial goal was the precise measurement of the beta-neutrino angular correlation coefficient in the decay of ${}^6\text{He}$. Its geometry results from a careful optimization of the harmonic potential created by cylindrical electrodes. It supersedes previously considered geometries that presented a smaller detection solid angle to the beta particle and the recoiling ion. We describe here the methods which were used for the potential optimization, and we present the measured performances in terms of trapping time, cloud size and temperature, and space charge related limits. The properties of the ion cloud at equilibrium are well reproduced by a simple numerical simulation using hard sphere collisions, which additionally gives insights on the trapping loss mechanism. The results of the numerical simulations and experimental measurements have been interpreted by a model whose justification is provided in a separate article. The open trap shall serve other projects. It is currently used for commissioning purpose in the TRAPSENSOR experiment and is also considered in tests of the Standard Model involving the beta decay of polarized ${}^{23}\text{Mg}$ and ${}^{39}\text{Ca}$ ion in the frame of the MORA experiment. The latter tests require in-trap polarization of the ions and further optimization of the trapping and detection setup. Based on the results of the simulations and of their interpretations given by the model, different improvements of the trapping setup are discussed.

Keywords: *Ion trapping, Ion cooling, correlation in nuclear β -decay, test of weak interaction*

1. Introduction

The LPCTrap experiment measures the β - ν angular correlation in the β decay of radioactive ions for tests of the Standard Model [1]. It uses a transparent Paul trap which allows the detection of the recoiling ion and beta particle in coincidence. As a rather natural extension of LPCTrap experiments carried out so far, the so-called *Matter's Origin from the RadioActivity of trapped and oriented ions* (MORA) project aims at measuring the CP violating D -triple correlation (see for example [2]) of laser-polarized ^{23}Mg and ^{39}Ca ions confined in an open Paul trap. Using such a laser-polarization technique in a LPCTrap-like setup would additionally enable precise measurements of other correlations involving oriented nuclei such as the beta asymmetry A_β or the neutrino asymmetry B_ν [2]. MORA will require the highest statistics to search for New Physics (NP) with the highest sensitivity. In this regard, the current open trap presents some limitations. In particular, the trapping lifetime is limited to a fraction of second, which causes unwanted losses and background events for the isotopes best suited to this measurement. After recalling the simple procedure which was followed to optimize the trapping of ions in the current open trap, the explanation for the short trapping times observed so far is being numerically investigated. Different methods for increasing the trapping time are then proposed for the D -correlation measurement.

2. The original open trap

In 3D Paul traps, ions are confined by means of a quadrupolar RadioFrequency (RF) potential [3]. In an “ideal” Paul trap, i.e. generating a pure quadrupolar potential, the trapping potential can be expressed using the (r, z) cylindrical coordinates in the following way:

$$(1) \quad V_{ideal}(r, z, t) = V_{rf}(t) \cdot \frac{r^2 - 2z^2}{2r_0^2}$$

where r_0 is a distance parameter, and $V_{rf}(t)$ is a sum of a Direct Current (DC) potential and Alternating Current (AC) potential. The DC component is usually used for a mass selective confinement, and reduces the trapping efficiency. For a non-mass-selective confinement, a pure AC potential is therefore preferred:

$$(2) \quad V_{rf}(t) = V_0 \cdot \cos(\Omega t).$$

where $\Omega = 2\pi\nu_{rf}$ is the angular radiofrequency. The potential in Eq. (1) is quite commonly approximated by electrodes whose surfaces form truncated hyperboloids, consisting of one ring and two end caps. These surfaces are represented in Fig. 1. In this configuration, the distance r_0 corresponds to the shortest distance from the trap center to the ring electrode, and $z_0 = \frac{r_0}{\sqrt{2}}$ corresponds to the distance to the end caps. Other geometries can approximate a pure quadrupolar potential. In full generality, the potential generated by a Paul trap consisting of electrodes of finite size and/or of approximated shapes can be expressed as an infinite sum of harmonics. In spherical coordinates (ρ, θ, φ) this gives:

$$(3) \quad V(\rho, \theta, \varphi, t) = V_{rf}(t) \cdot \sum_{n=0}^{\infty} \sum_{m=-n}^n C_{nm} \left(\frac{\rho}{r_0}\right)^n P_n^m(\cos \theta) e^{im\varphi}$$

where the complex harmonic coefficient C_{nm} represents the respective strengths of the multipoles (n, m) , and $P_n^m(\cos \theta)$ is the associated Legendre polynomial of order m and degree n . The effect of the multipoles of order higher than 2 is to create instabilities in the ion motion, leading the ions out of the trap (see for example [4]). Different geometries of Paul traps were studied and compared to optimize the trapping performances for the measurement of the β - ν angular correlation in the ${}^6\text{He}$ β decay (see Fig. 2): a transparent trap using wires to form hyperboloidal surfaces [5], a trap made of 6 rings [6] and a simple cylindrical trap presented and compared to the other geometries in [7].

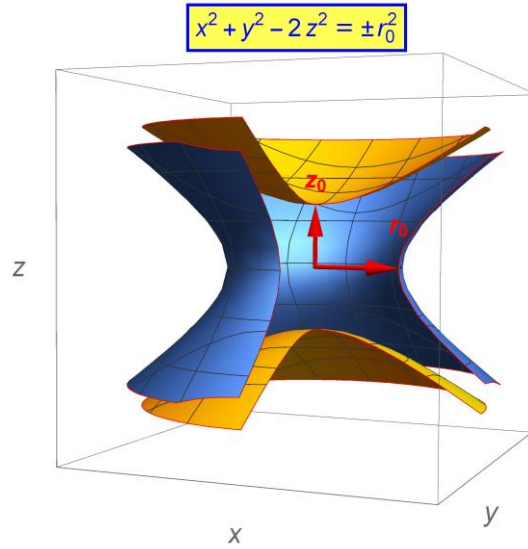


Figure 1 : Hyperboloids commonly used for the geometry of electrodes in 3D Paul traps. The distances of the ring and end cap electrodes to the center of the trap are respectively called r_0 and z_0 . They are related by the formula: $z_0 = \frac{r_0}{\sqrt{2}}$.

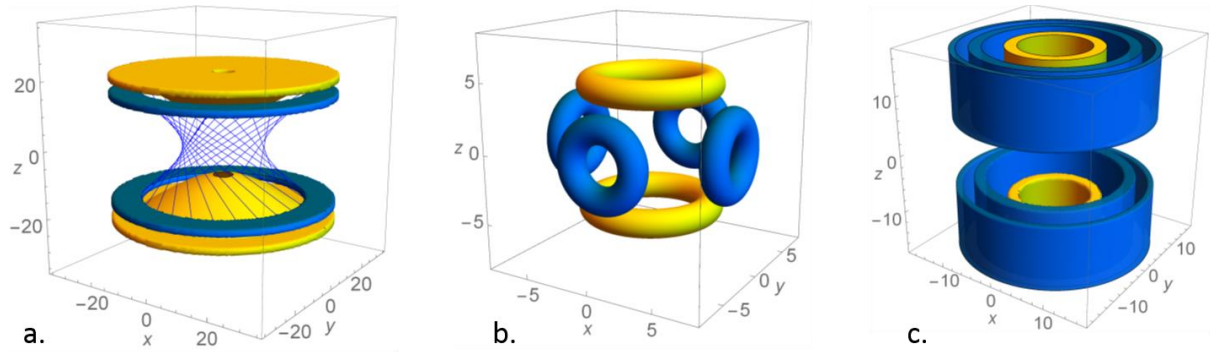


Figure 2: Geometries originally considered for the open trap of LPCTrap. Dimensions are in mm. The electrodes mimicking the ring of Fig. 1 are shown in blue, the ones mimicking the end caps are shown in yellow. Inset a.: Paul trap whose ring was made of wires [5]. This design was inspired from a setup used at Ayme Cotton Laboratory by J. Pinard. Inset b.: trap made of rings studied in [6], inspired from a design found in [8]. Inset c.: the so-called “tube trap” [7], which was developed and finally adopted for LPCTrap.

The so-called “tube trap” was preferred because of its higher transparency and simplicity. In such a trap, the axial symmetry and the planar symmetry reduce the multipole expansion of the potential of Eq. (3) to a sum of zero order ($m = 0$) and even degree ($2n$) associated Legendre polynomials, respectively:

$$(4) \quad V(\rho, \theta, t) = V_{rf}(t) \cdot \sum_{n=0}^{\infty} A_{2n} \left(\frac{\rho}{r_0} \right)^{2n} P_{2n}(\cos \theta)$$

where the coefficient A_{2n} are given by $A_{2n} = \mathbb{R}e(C_{2n0})$, and the $P_{2n}(\cos \theta) = P_{2n}^0(\cos \theta)$ are Legendre polynomials of degree $2n$. In cylindrical coordinates, Eq. (4) can be rewritten as a sum of polynomials of even degrees in r and z :

$$(5) \quad V(r, z, t) = V_{rf}(t) \cdot \sum_{n=0}^{\infty} H_{2n}(r, z) = V_{rf}(t) \cdot \sum_{n=0}^{\infty} \frac{A_{2n}}{r_0^{2n}} \sum_{k=0}^n a_{2k}^{2(n-k)} r^{2k} z^{2(n-k)}$$

where the a_i^j coefficients are defined by the following recurrence relation to satisfy the Laplace equation:

$$(6) \quad a_{i-2}^{j+2} = -\frac{i^2}{(j+1)(j+2)} a_i^j \text{ with } a_{2n}^0 = P_{2n}(0)$$

Using Eq. (5) and (6), we observe that $V_{ideal}(r, z, t) = V_{rf}(t) \cdot H_2(r, z)$. The geometry of the trap is shown in detail in Fig. 3. In this geometry, the central tubes are mimicking the end cap electrodes of Fig. 1. The equipotential lines shown are calculated by SIMION [9] for 1 V set on these electrodes. The size and position of the tubes, shown in Fig. 3, were finely tuned to favor the formation of a quadrupolar potential, thus minimizing the multipoles of higher order: $H_2 \gg H_{2n} \forall n > 1$ in the region of interest. The inset i of Fig. 4 is a zoom on the potential created in the central region of the trap, delimited by the large dashed rectangle (B) in Fig. 3. The reference potential is taken at the center of the trap. A chi-square adjustment of potential of the form of Eq. (5) yielded the harmonic coefficients as shown in Tab. 1.

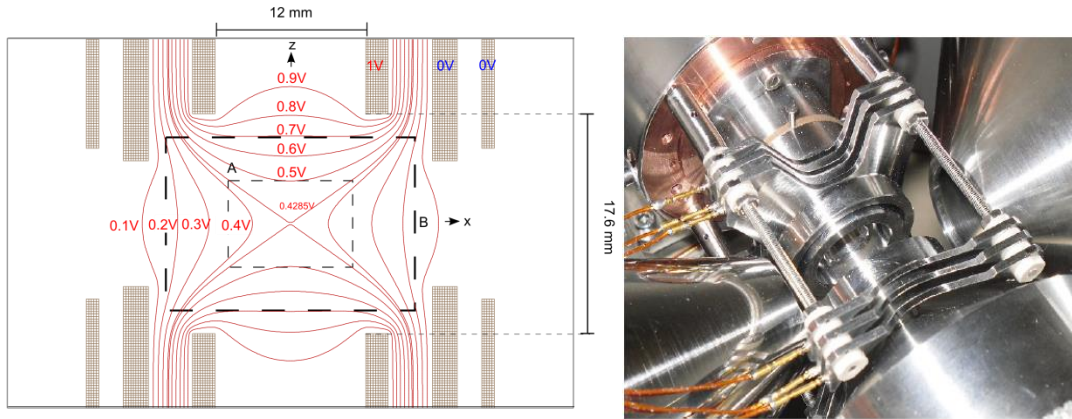


Figure 3 : Geometry of the open Paul trap. Left inset: cross section of the trap and equipotential lines as calculated by SIMION. The z-axis is the axis of revolution of the trap. The distance between the electrodes mimicking the end caps is 17.6mm, so that $z_0 \approx 8.8\text{mm}$. Right inset: photograph of the real arrangement of the trap.

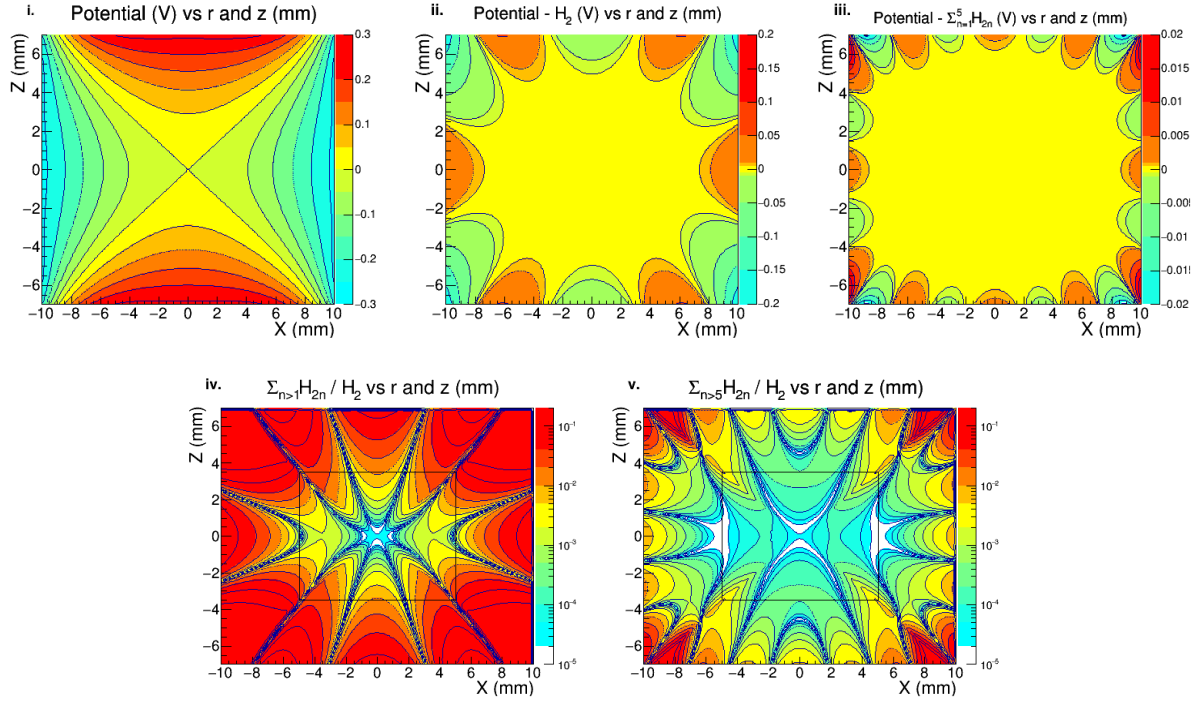


Figure 4 : Inset i: potential created by the electrodes in the configuration of Fig. 3. Insets ii and iii: residuals resulting from the subtraction of the different sum of multipoles to the potential of inset i. Insets iv and v: corresponding relative residuals, normalized to H_2 . The black rectangles show the region discussed in the text, corresponding to the small dashed rectangle (A) in Fig. 3.

Multipole	Quadrupole	Octupole	Dodecapole	16 - pole	20 - pole
r_0 (mm)	$A_2(V)$	$A_4(V)$	$A_6(V)$	$A_8(V)$	$A_{10}(V)$
12.875 ± 0.069	1	-0.102 ± 0.003	-0.90 ± 0.02	-0.0661 ± 3	0.51 ± 0.01

Table 1 : Coefficients of the main harmonics of the open trap potential.

The distance parameter r_0 in Table 1 is consistent with a rough estimate from the distance of the central tube tips to the center of the trap (Fig. 3): $r_0 = z_0 \cdot \sqrt{2} \approx 8.8 \times \sqrt{2}$ mm. Residual fields obtained after subtracting the quadrupolar field alone and the sum of harmonics as given in Table 1 are shown in the insets ii and iii. They are normalized to the H_2 multipole in insets iv and v. As can be seen in the inset iv, the contributions of the octupolar and dodecapolar harmonics are dominant in the rim of the region of interest, and decrease when approaching the trap center. Their relative contribution to the potential is below 2-3 % in a region delimited by $r = \pm 5$ mm, $z = \pm 3.5$ mm around the center of the trap (black rectangle in the inset iv). In the same region, the maximal contribution of higher order multipoles (inset v) is in the order of 0.3 %. With such trap, a trapping lifetime ranging from 100 ms to 500 ms was experimentally observed [1]. The trapping losses are attributed to ion – neutral collisions and electric field imperfections [10]. The cloud temperature was determined to be of the order of 0.1 eV and the size of the order of 2.4 mm FWHM for ^6He [1,11]. A space charge capacity of the order of $2.5 \cdot 10^5$ ions per bunch was observed with ^{39}K [1]. For the purpose of future experiments, it is worthwhile to investigate the origin of the trapping losses, as well as possible ways of reducing the cloud size and temperature. These latter are indeed the dominant sources of systematic uncertainty on the β -v angular correlation parameter [1,11], and in turn will certainly matter in the D -correlation measurement.

3. Numerical investigations of the trapping performances

The trapping performances were investigated numerically using the expression of the potential as formulated in Eq. (5), and a Bulirsch-Stoer integration method [12] combined with a hard sphere collision model to integrate the ion motion differential equations. As a crude estimate, a geometrical collision cross section of $4\pi a_0^2$ was used, with a_0 corresponding to the Bohr radius, as no mobility data exists for the experimental conditions presented here: $E/N > 10^6$ Td [13], where E refers to the electric field and N to the neutral gas concentration. Such a simple approach is meant to give qualitative results and is compared for consistency to experimental data presented in [1,11]. The work presented here will be followed by a more detailed study using the simulation package developed for the analysis of the β - v angular parameter [14], which is able to account for space charge effects and different realistic ion – neutral interaction potentials.

3.1 Test cases

As a reference study, $^{39}\text{K}^+$ ions for which experimental data exists at LPCTrap [1] are considered. Ions are injected in the trap center with a small spatial spread $\sigma_x=\sigma_y=\sigma_z=0.1$ mm and a quite typical energy spread from a RFQ cooler buncher: $\sigma_E \approx 1$ eV. Even tiny, such a phase - space volume overcomes the phase – space capacity of the trap, as a large fraction of the ions (>50% in the most favorable cases) is lost in the first μs . Ions are considered as lost when their trajectory crosses the border of the region shown in Fig. 3, entering areas close to the electrodes where high order harmonics ($2n \geq 10$) dominate, or of a downscaled region for the study of the effective trapping area as detailed in the next section. In the following, the ideal potential refers to a pure quadrupolar potential based on the r_0 and A_2 values of Table 1, while the realistic potential additionally includes the higher order harmonics up to $2n=10$. When the hard sphere collision model was used, an arbitrary high residual pressure of $5 \cdot 10^{-4}$ mbar of He gas was assumed, using the geometrical cross section as defined above for estimating the probability of collision. Unless specified otherwise, an ambient gas temperature of 300 K was generally adopted. In these conditions, the collision frequency was kept rather high (of the order of 1 kHz) to limit the computation time, but well below the ion macro-motion frequency, yielding results which are scalable with the lower pressures usually used at LPCTrap, and/or with more realistic collision cross sections. In the results detailed in the following, the ion cloud phase – space reaches a steady state after a few 10 μs only when no collisions are applied, and after a few 10 ms (about 30 collisions) when buffer gas cooling is applied. The trapping of $^{39}\text{K}^+$ ions was considered for a variable RF voltage and a fixed frequency of 600 kHz. Doing so, the stability diagram [3] was scanned for Mathieu parameter q_z ranging from 0.14 to 0.83, where

$$(7) \quad q_z = \frac{4qV_0}{mr_0^2\Omega^2}$$

with m and q the mass and charge of the ions.

The motion in an ideal Paul trap is stable for $q_z < 0.908$, condition which could be numerically verified. For each individual set of parameters, the trajectories of an ensemble of 1500 ions were calculated for trapping times up to 500 ms.

3.2 Results

3.2.1 Effective trapping region

Away from the trap center, harmonics of order larger than 2 will progressively make the real potential depart from the ideal one, eventually yielding instabilities for the ion motion, as a result of non linear resonances in the stability diagram ejecting ions from the trap (see for example [4]). In order to

estimate the effect of the departure from the ideal potential on the trapping efficiency, the loss criterion described above, *i.e.* $r > 10$ mm and $|z| > 10/\sqrt{2}$ mm, corresponding to the border of the region shown in Fig. 4, was systematically downscaled by steps of 1 mm down to $r > 2$ mm and $|z| > \sqrt{2}$ mm. This loss criterion was applied to ions either injected in the ideal or in the real potential. For these simulations the buffer gas cooling was not applied. The result of this systematic investigation is shown in Fig. 5 for a Mathieu parameter $q_z=0.277$, where $^{39}\text{K}^+$ ions were considered as trapped when they were still flying after an arbitrary time of 10 ms: in the absence of collisions, it was in fact observed that the ion losses essentially occur in the first 50 μs following the injection in the trap, while after a flying time of about 100 μs most of the trapped ions remain indefinitely in the trap. As can be observed in Fig. 5, the number of trapped ions for the real and ideal potentials is very similar up to a radius of about 5 mm, indicating that for ions whose initial trajectory is contained in the corresponding region of space, the motion remains indefinitely stable. Beyond this radius, the real potential fails to trap the ions. A very similar behavior was found for other Mathieu parameters, showing that the effective trapping area of the real Paul trap is limited to a region of radius $r_{eff} \approx 5$ mm and axial size $z_{eff} = \frac{r_{eff}}{\sqrt{2}} \approx 3.5$ mm around the center of the trap, irrespective to the value of V_0 . The reduction of the size of the trapping area is a direct consequence of the high order harmonics, whose effect starts being non negligible when their contribution becomes greater than a couple of percents.

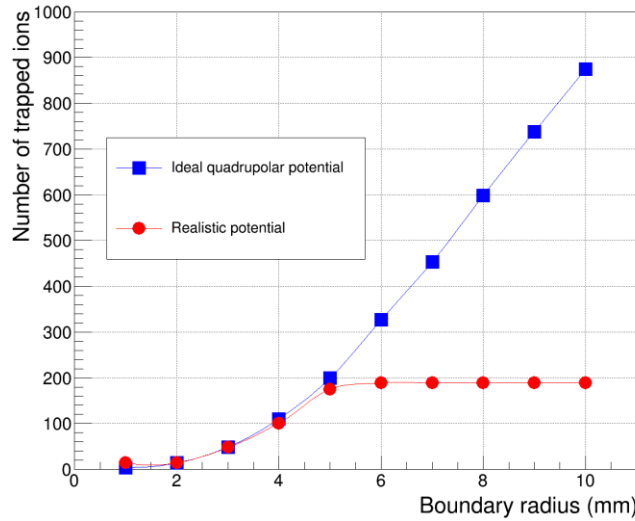


Figure 5 : Number of trapped ions after a flying time of 10 ms versus the radius of the trap boundary for an ideal field and for a realistic field. In these simulations no collisions were considered.

3.2.2 Interpretation of the buffer gas cooling and phase - space evolution

The finite boundary of the effective trapping area is expected to have some implication on the maximal energies of ions which are stored in the trap. In Paul traps, it is customary to decompose the ion motion in so-called macromotion and micromotion:

$$(8) \quad z = Z + \delta$$

Where Z refers to the secular motion, also commonly called macromotion, and δ to the micromotion. This approximation is well established for relatively low q_z values, for which a pseudo-potential well can be calculated [3]. The depth of this pseudo-potential for an ideal trap reads

$$(9) \quad D_r = \frac{q_z \times V_0}{16}$$

in the radial direction and

$$(10) \quad D_z = \frac{q_z \times V_0}{8} = 2D_r$$

in the axial direction. For a real trap, V_{eff} is defined as the amplitude of the RF potential at the rim of the effective trapping region, where the quadrupolar potential is still dominating. Recalling that $r_{eff} \approx 5$ mm is the radius delimiting this region, we get

$$(11) \quad V_{eff} = V_0 \left(\frac{r_{eff}}{r_0} \right)^2$$

Under these conditions one can define the associated effective pseudo-potential depths which correspond to the maximal energies of ions that can be effectively trapped [3]

$$(12) \quad D_{zeff} = D_z \left(\frac{r_{eff}}{r_0} \right)^2 = 2D_{reff}$$

In the present case, $\left(r_{eff}/r_0 \right) \approx (5/12.9)^2 = 0.15$, so that the effective pseudo-potential depths are significantly reduced compared to an ideal trap. In such conditions, it is probable that the relatively short trapping lifetimes observed with LPCTrap are caused by ion evaporation from the shallow potential of the trap. More precisely, collisions may be boiling off ions from the trap when their trajectories bring them beyond the effective trapping region. This hypothesis was confirmed in an analytical study of the cloud properties reaching a thermal equilibrium with the neutral gas. The model is presented in a separate article [15] as it is not restricted to LPCTrap but generally applies to all Paul trap systems where ions are cooled down by collisions. It is based on the pseudo-potential approximation and applies to relatively low q_z values. Ion-atom collisions are approximated by hard sphere collisions, in the similar fashion as was done in the simulations. We recall here some of the results which we will use in the following.

Assuming that the cooling rate is much faster than the evaporation rate, one can define an effective equilibrium temperature T_{eff} for the ion cloud for relatively small q_z values. Calling $\overline{E_k}$ is the average energy of the ions over the cloud phase space and RF period, T is the temperature of the buffer gas, and m_g is the mass of the buffer gas molecule, it was found that

$$(13) \quad \overline{E_k} = \frac{3}{2} k T_{eff} \approx \frac{3kT}{1 - \frac{m_g}{m}}$$

so that $T_{eff} \approx \frac{2T}{1 - \frac{m_g}{m}}$.

$\overline{E_k}$ is related to the average squared radius $\overline{\rho^2}$ and the radial distribution root mean square σ_r via the relationships:

$$(14) \quad \overline{E_k} \approx \frac{8eD_r}{3} \cdot \frac{\overline{\rho^2}}{r_0^2} = 6eD_r \cdot \frac{\sigma_r^2}{r_0^2}$$

One can define a cooling half period which corresponds to the average number of collisions required to reduce velocities beyond the thermal bath by a factor of about 2:

$$(15) \quad n_{1/2} \approx \frac{m}{\mu} \ln(2)$$

A complete cooling is achieved after about 5 half periods.

Finally it is shown that the rate of evaporation of ions from the ion trap primarily depends on the ratio between the pseudo-potential effective depths to the thermal energies denoted $\alpha_{Ez} = \frac{D_{zeff}}{kT_{eff}}$ and $\alpha_{Er} = \frac{D_{reft}}{kT_{eff}}$, and an approximate formula for the trapping lifetime is derived.

In the following the results of the simulation are discussed, and interpreted thanks to the model. They are compared to the experimental results. Possible ways of optimizing the trap performances for the MORA project are eventually discussed.

3.2.3 Temperature and mean radius of the ion cloud

Figure 6 presents an example of evolutions of the mean ion cloud kinetic energy and radii for ions trapped and cooled by a buffer gas of He at different q_z parameters. Realistic potentials with harmonics $2n>2$ were used. The energies and radii are averaged over several RF cycles. The fluctuations of the mean radius which can be observed for $q_z=0.28$ are due to the relatively small statistics for this parameter. In the conditions of the simulation ($P_{He} = 5 \cdot 10^{-4}$ mbar, using the aforementioned geometrical cross section), the cloud takes about 50 ms to thermalize completely. This corresponds to about 30-40 collisions, which amounts as expected to roughly 5 cooling half periods as given by Eq. (15). In the left inset of Fig. 6, the energies corresponding to the temperatures of the model (Eq. (13)) and of the Brownian motion corresponding to a gas temperature of 300 K are materialized by dashed lines. The mean kinetic energies for q_z values up to 0.55 tend to match the one of the model after complete cooling. The temperature of equilibrium of ions is higher than the temperature of the buffer gas, as a result from the so-called RF heating effect [16]. The use of cryogenic traps at liquid He or N temperature drastically reduces the energies and radii of the trapped ions. In the right inset of Fig. 6, it is interesting to observe that a higher q_z value, or equivalently higher RF voltage, also yields significantly smaller radii, while the mean energy does not increase in the same proportion, when $q_z \leq 0.55$.

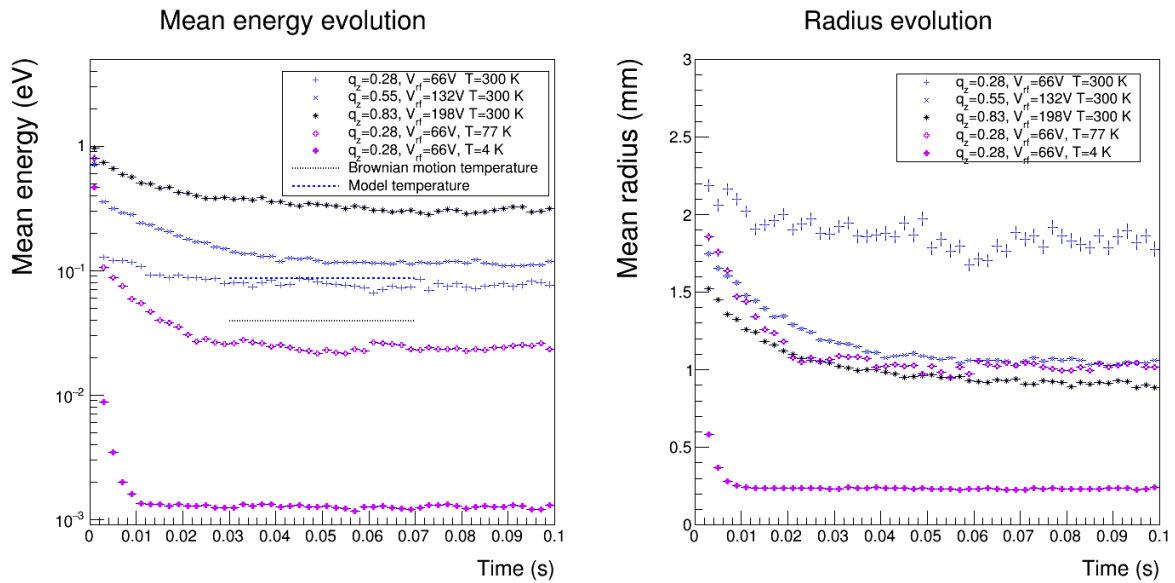


Figure 6 : Phase - space evolution of the ion cloud. Left: average ion kinetic energies for different Mathieu parameters and gas temperature. The theoretical average energy for a Brownian motion at 300 K (~ 39 meV) is shown by a dashed line for comparison, as well as the average energy corresponding to $T=300\text{ K}$ from the model developed in [15]. Right:

average ion radius to the center of the trap for different Mathieu parameters (and corresponding RF voltages) and gas temperature. See text for more explanations.

Figure 7 shows a comparison of the mean kinetic energies obtained by simulation to the ones of the model (Eq. (13)) for a buffer gas at room temperature for a wider range of Mathieu parameter. For $q_z \leq 0.2$ the energies of the trapped ions are limited by the small depth of the pseudo-potential well. Under such conditions the evaporation rate is large and the lifetime of ions in the trap does not exceed a couple of collisions. For high q_z values ($q_z \geq 0.6$) the mean energies depart from the model as the validity of the pseudo-potential approximation is fading out. For these values, the ion motion includes other harmonics than the simple decomposition in macro- and micromotions of Eq. (8), resulting in a hotter effective temperature. The mean energies are still relatively well related to the ion radius via Eq. (14). There is still a large region for which the model gives a good approximation of the effective temperature: $0.2 \leq q_z \leq 0.6$, which practically covers the domain for which the best performances are obtained for most traps, including LPCTrap. For cryogenic temperatures, the evaporation rate is strongly inhibited by the large α_{Er}, α_{Ez} ratios. Under these conditions, the agreement of the model with the simulation is excellent even with relatively low q_z values, as shown in Fig. 8. Figure 9 presents the average squared radii for different q_z values as simulated, and predicted by the model. As the average squared radii are related to mean energies by Eq. (14), similar observations than those aforementioned for the energies can be made. For low q_z values ($q_z \leq 0.2$), the high evaporation rate results in reduced mean kinetic energy and therefore reduced squared radii. For high q_z values ($q_z \geq 0.6$), other harmonics than the ones giving rise to the macro- and micromotions have to be included in the ion motion, resulting in a hotter temperature and therefore larger squared radii. Again, the agreement with the model is good on the region $0.2 \leq q_z \leq 0.6$.

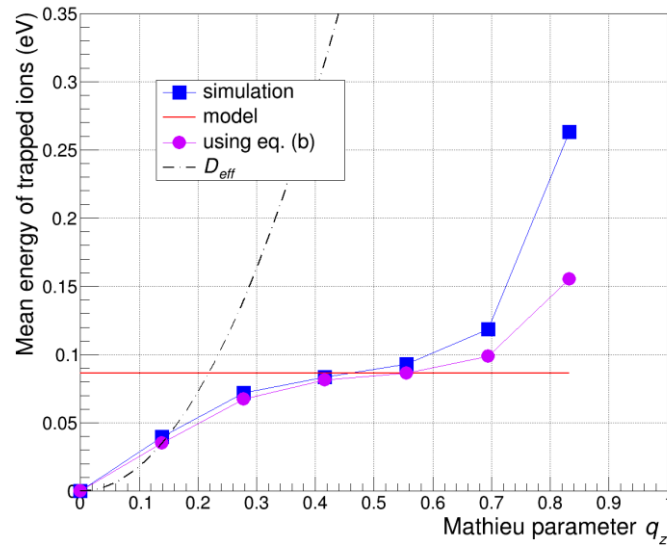


Figure 7 : Mean kinetic energy from simulations, model (Eq. (13) and (14)), and injecting the simulated average radii in Eq. (14). At low q_z values the mean kinetic energy is limited by the weakness of the pseudo-potential. At high values the validity of the pseudo-potential approximation is fading out. See text for more details.

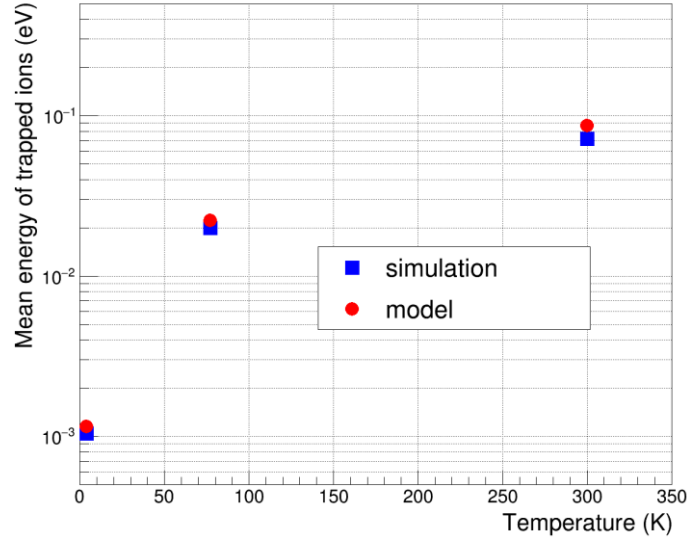


Figure 8 : Comparison of the mean energies of ions from the model and simulations for a q_z value of 0.28 at different temperatures.

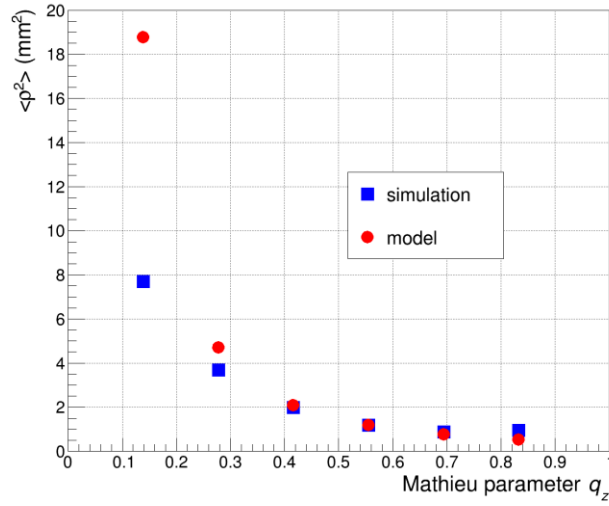


Figure 9 : Average squared radius vs q_z , as estimated from the model (Eq. (13) and (14)), and calculated with the Monte Carlo simulations.

3.2.4 Trapping lifetime

Figure 10 shows an example of lifetime plot obtained for an RF voltage of 66 V, corresponding to $q_z=0.28$. When no cooling is applied, most ions which are stable for the first 100 μ s remain stable over the 500 ms of the simulation, in accordance with the observations done when determining the effective trapping region (see Sec. 3.2.1). When cooling is applied (gas at 300 K), ions are getting lost with time. These losses disappear in the case of a cryogenic Paul trap at 77 K or 4 K. The 4 K trap even enhances the trapping efficiency of ions freshly injected in the trap.

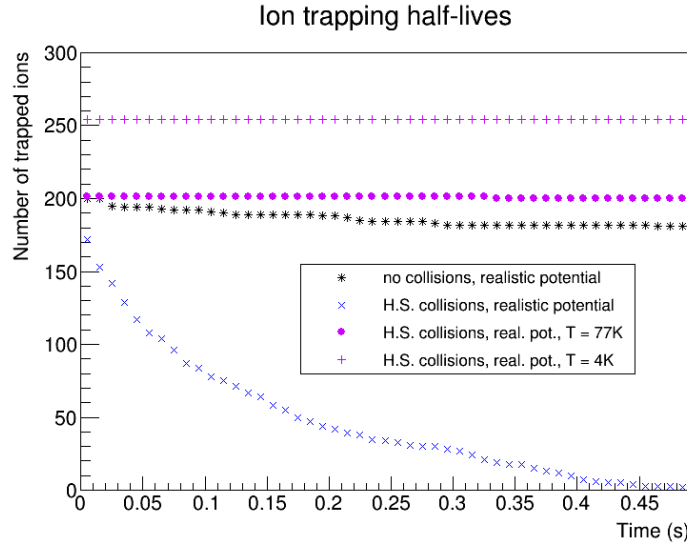


Figure 10 : Time evolution of the number of trapped ions.

The trapping lifetimes expressed in terms of number of collisions have been determined by simulations for a number of RF voltages, as shown in Fig. 11. For the shortest lifetime, the error bars correspond to fluctuations observed for simulations repeated with different starting temperatures. The analytical model gives rather accurate predictions: we used here Eq. (66) from ref. [15] with an effective radius of $r_{eff} = 4.5$ mm which was found to best match the data. This radius is consistent with the dimensions found for the effective trapping area $r_{eff} \approx 5$ mm, and corresponds to the limit at which the curve connecting the blue squares of Fig. 5 departs from the one connecting the red disks. For too high q_z values ($q_z \geq 0.5$) the lifetime is so large that it becomes difficult to evaluate by simulations. As stated above, the lifetime as deduced from the model primarily depends on the ratio of the maximal confined ion energy to the thermal energy in the trap $\alpha_{Er} = \frac{D_{refff}}{kT_{eff}}$ also plotted in Fig. 11. This ratio can be efficiently increased, and the evaporation rate drastically reduced, either by increasing the RF voltage (and therefore D_{refff}) or by reducing the temperature of the trapped ions by using gases at cryogenic temperatures.

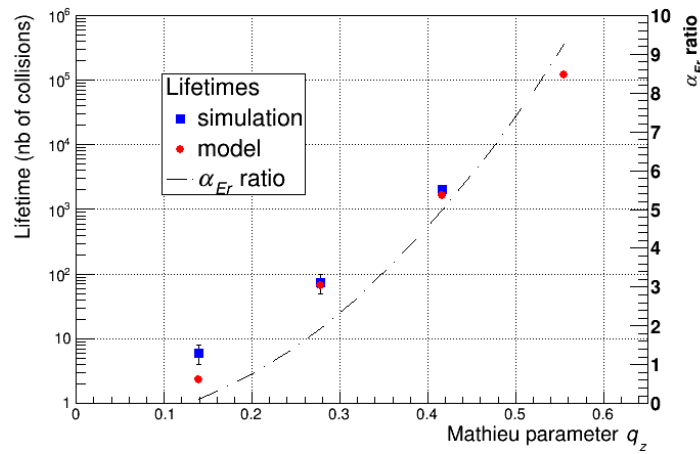


Figure 11 : Trapping lifetime, expressed in number of collisions, as obtained from Monte Carlo simulations and from the model developed in Ref. [15]. The ratio $\alpha_{Er} = \frac{D_{refff}}{kT_{eff}}$ on which the lifetime primarily depends is also plotted as the dash line.

3.2.5 Comparison with experimental results

The simulation results have been compared with two systems: buffer gas cooling of ${}^6\text{He}$ and ${}^{39}\text{K}$, reported for example in Refs. [1] and [11]. In Ref. [11], the radial dimensions and the energy distribution of the ${}^6\text{He}$ cloud are inferred from the measurement of recoil ion time-of-flight of ${}^6\text{Li}^+$ ions extracted from the trap and its comparison to simulations using realistic collision potentials, as detailed in Ref. [17]. As can be seen in Fig. 12, the simulations presented here yield an rms radius for the radial dimensions of the cloud of $\sigma_x = \sigma_y = \sigma_r = 1.19$ mm. This value is in almost perfect agreement with the value r^2 of 1.5 mm^2 shown in Refs. [1] and [11]. The rms deviation in z is twice lower than in the radial dimensions, as expected by the model. The mean energy, of 0.10 eV, is both in good agreement with the value of 0.09 eV obtained from simulations using realistic potentials shown in Ref. [17], and the experimental one which was found to be slightly larger, of $0.107(7)$ eV. With a rather low α_{Er} ratio ($\alpha_{Er} = 2.1$), the evaporation of ${}^6\text{He}^+$ ions cannot be completely neglected. The analytical model, which does not take into account the evaporation from the trap, gives as expected slightly higher values for the mean energy and rms deviation than observed and simulated: A mean energy of 0.116 eV and an rms radius of 1.38 mm could be calculated.

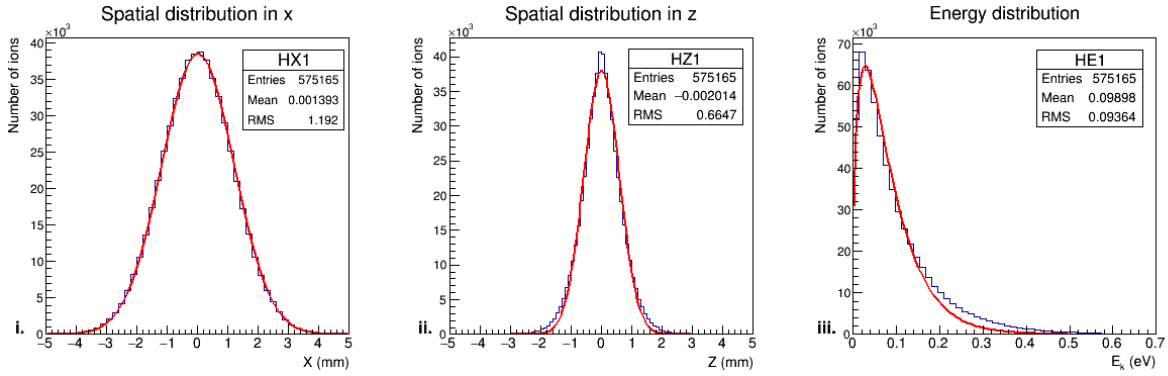


Figure 12 : From left to right: distributions along (i) the radial x dimension (ii) the axial dimension and (iii) as a function of the kinetic energy for ${}^6\text{He}$ trapped with $V_{rf}=60\text{V}$, $\Omega_{rf}=1.15\text{MHz}$. Results of a Gaussian fit and of a Maxwell-Boltzmann distribution in red are superimposed for a comparison of the assumptions of the analytical model developed in Ref. [15]. The distribution in y is not shown as it is very similar to (i).

These comparisons show that despite its apparent simplicity, the hard sphere collision simulations and the associated model are quite accurate in describing the cloud at equilibrium in the trap. They give results which are consistent with the experimental observations of the ion cloud properties (size and energies), and with a simulation using realistic potentials for describing the collisions. A similar observation was done in Ref. [14].

Because it yields correct equilibrium states, the hard sphere approximation is expected to give a correct qualitative description of the ion evaporation process and of the trapping efficiency as described in the previous sections. In fact, the main limitation of the such approach comes from the lack of precise knowledge of an effective hard sphere cross section. The geometrical cross sections used here are crude estimates which yield equilibration times such as the trapping half-life, or cooling times which are found to be overestimated by one to two orders of magnitude. In Ref. [1], typical trapping half-lives of 500 ms are reported for all ion species. As an alkali ion, ${}^{39}\text{K}^+$ does not likely recombine with surrounding atoms or molecules, so that the observed trapping half-life will essentially be due to the evaporation of ions agitated by collisions with the residual gas out of the effective

trapping area, as described by the simulations and the model. The comparison between the theoretical trapping half-life predicted by simulations presented here with the experimental one permits therefore to obtain a better estimate of the effective hard sphere cross section. With a residual gas pressure of $2 \cdot 10^{-6}$ mbar, the simulated trapping half-life for the radiofrequency parameters typically used (600 kHz, $V_0 \approx 66$ V, which are the same parameters as used in Fig. 10) this comparison yields an effective hard sphere cross section of $1.6 \cdot 10^{-18}$ m², above the geometrical one by a factor close to 50. Such order of magnitude is in the range of values that can be found for other systems at higher pressures in Ref. [13]. It is consistent with a longer range interaction as can be predicted for realistic potentials [14,18]. A comparison of the results of the model and simulations with the cooling time of the ${}^6\text{He}^+$ ion cloud reported in Ref. [11] leads to a similar conclusion: the simulation is consistent with the model, but again overestimates by approximately 2 orders of magnitude the observed cooling time, so that the effective hard sphere cross section for this system has to be of the order of $3 \cdot 10^{-18}$ m².

With these results, some conclusions can be drawn for the realization of future experiments, where a fine control of the properties of the ion cloud (size and energies) and best performances in term of capture and trapping times are desired. This is particularly the case for the MORA project.

4. Prospects for the MORA project

LPCTrap provided new data on the β - ν angular correlation in the decay of ${}^6\text{He}$, ${}^{35}\text{Ar}$ and ${}^{19}\text{Ne}$ [1,19]. These experiments are currently being analyzed. The ${}^6\text{He}$ data should permit to set competitive constraints on the existence of tensor currents. The ${}^{35}\text{Ar}$ and ${}^{19}\text{Ne}$ data should permit to improve the determination of the first element of the CKM matrix, V_{ud} , from mirror nuclides. As a rather natural extension of the physics program of LPCTrap, the measurement of the triple correlation D is one of the most promising experiments to search for New Physics. The D correlation is a triple correlation of the form $D \frac{\langle \vec{J} \rangle}{J} \cdot \left(\frac{\vec{p}_e}{E_e} \cdot \frac{\vec{p}_\nu}{E_\nu} \right)$ where J is the nuclear spin, E_e , p_e and E_ν , p_ν are the momenta and total energies of the electron and neutrino, respectively. The D correlation violates Time reversal symmetry, and via the CPT theorem, is sensitive to CP violation. The principle of the measurement of the D correlation, undertaken in the frame of the MORA project, will be detailed in a forthcoming publication [20]. The D -correlation will be measured using a similar arrangement as for the β - ν angular correlation, with recoil ion and β detectors in the azimuthal plane of the trap. ${}^{23}\text{Mg}$ and ${}^{39}\text{Ca}$ isotopes will be laser polarized in the trap as ions, as done at β -NMR setups like COLLAPS (see eg [21, 22]). In the trap, it is expected that the achievable polarization degree would be close to 100%. Considering the half-lives of ${}^{23}\text{Mg}$ and ${}^{39}\text{Ca}$, of 11.3 s and 860 ms respectively, the short trapping lifetimes (100-500 ms) observed with the LPCTrap setup would be either a source of unwanted background or of unwanted losses for the D -correlation measurement. Considering the low ${}^{39}\text{Ca}$ production rate from ISOL facilities, a good trapping efficiency is particularly desired for this ion. For both isotopes, it has been found that a mean kinetic energy of 0.1 eV would be hindering the spin orientation of the isotopes if continuous lasers had to be used. Such lasers which would have a bandwidth much smaller than the Doppler broadening of the transitions of interest (typically 200 MHz as compared to 5 GHz). The use of pulsed lasers of much broader bandwidth is therefore considered as an advantageous alternative. Nevertheless, a lower kinetic energy and corresponding smaller radii could speed up and render more efficient the nuclear orientation, at least by concentrating the laser flux on a smaller region of space. For these reasons a more efficient cooling mechanism than presently used at LPCTrap could also be envisaged.

Using the results of the numerical study and of the model detailed in Sec. 3, the experimental trapping lifetime which was found to be of the order of 500 ms, could be extended to a few seconds in two ways (see Fig. 11 and discussion of the importance of the α_{Er} , α_{Ez} factors):

- Increasing the depth of the effective pseudo-potential well by
 - using a higher RF voltage, and/or
 - extending the effective trapping area
- Cooling the ion cloud down to cryogenic temperatures

Both options would additionally permit to trap more efficiently freshly injected ions (Sec. 3). Nevertheless, increasing the RF voltage alone to increase the depth of the effective pseudo-potential well would have an unwanted side effect: the maximal recoiling energy of the ^{23}Mg ions being of the order of 300 eV only, a higher RF field would disturb more the recoil ion trajectories than a lower field. This would result in comparably higher systematic effects [11] to be cared for in the analysis of the experimental data and a possible washout/loss of sensitivity of the D -correlation measurement. In this respect it is much more advantageous to extend the effective trapping area, by fine tuning the shape of the transparent Paul trap in order to suppress even further the contribution of harmonics of degrees larger than 2. This optimization is actively undertaken by the MORA collaboration using methods more sophisticated than presented in Sec. 2, which will be detailed in future publications.

Cryogenic Paul traps have already been built for different purposes (see for example [23,24]) and could eventually be considered for the D -correlation measurement, in case for instance the Doppler broadening arising from the thermal agitation and RF heating of ions trapped at room temperature is found unacceptable for the nuclear orientation. Alternatively, the use of sympathetic cooling could be envisaged. The laser cooling of Ca^+ ions in a trap very similar to LPCTrap was recently demonstrated for the TRAPSENSOR project [25,26]. $^{23}\text{Mg}^+$ or $^{39}\text{Ca}^+$ ions could then be cooled by collisions with laser cooled Ca^+ ions. This cooling scheme will be studied by the TRAPSENSOR team.

5. Conclusion

The open LPC Paul trap uses a simple geometry which has been optimized in order to minimize the contribution of non quadrupolar harmonics in an extended region of the electrodes inner space. The design has been successful for performing the β - v angular correlation measurements at GANIL, and is now further used for the commissioning of the TRAPSENSOR project. An optimization of the trap is being undertaken for a measurement of the D correlation in the beta decay of oriented nuclei in the frame of the MORA project. Simulations have been carried out to understand the present limitations, and an analytical model of the ion cloud properties was derived. The numerical studies have shown that the potential harmonics of order larger than 2 were limiting the trapping region dimensions to a radius of 5 mm around the trap center. Following this finding, the model which was derived shows that ions are evaporated from the trap because of collisions with the residual gas bringing them to the boundary of the trapping region. This effect is more pronounced for lower RF voltages as the depth of the effective pseudo-potential becomes too small compared to the thermal agitation of the ion cloud. Such a process is therefore pinpointed to be the principal cause of the observed trapping losses. For the MORA project, the optimization of the trap which is presently being undertaken consists in enlarging the effective trapping area by fine tuning the shape of the electrodes. The resulting enlarged depth of the effective pseudo-potential should permit to reduce efficiently the trapping losses. In

principle, the use of buffer gas cooling at cryogenic temperature would additionally permit achieving indefinitely long trapping times, while reducing efficiently the width of the ion cloud energy distribution. Another cooling method which is being investigated by the TRAPSENSOR team is the sympathetic cooling with laser cooled Ca^+ ions. Both cooling techniques could equally be considered for the MORA project, if the efficiency laser orientation technique would be proven not to be effective enough (<50%) for the D -correlation measurement.

6. Acknowledgements

The authors acknowledge the support from Region Normandie for the MORA project.

7. References

- [1]: G. Ban et al, Ann. Phys. (Berlin) 525, N° **8-9**, 576 (2013).
- [2]: M. Gonzalez-Alonso, O. Naviliat-Cuncic and N. Severijns, [arXiv:1803.08732](https://arxiv.org/abs/1803.08732) [hep-ph], accepted in Progress in Particle and Nuclear Physics (2018).
- [3]: R. E. March, J. F. J. Todd, Quadrupole Ion Trap Mass Spectrometry, Chemical Analysis, a series of monographs on analytical chemistry and its applications, Series Editor J. D. Winefordner, Wiley, 2005.
- [4]: R. Alheit, C. Henning, R. Morgenstern, F. Vedel and G. Werth, Appl. Phys. B **61**, 277 (1995).
- [5]: P. Delahaye et al, Hyp. Int. **132**, 475 (2001).
- [6]: P. Delahaye, PhD thesis of the University of Caen Basse-Normandie, 2002.
- [7]: P. Delahaye et al, *a new Paul trap geometry for a measurement of $\beta - \nu$ angular correlation in ^6He decay*, poster presented at the HCI Conference, Caen, 2002.
- [8]: P. H. Dawson, Quadrupole Mass Spectrometry and its Applications, American Vacuum Society Classics, 1976
- [9]: D. Manura, D. Dahl. SIMION (R) 8.0 User Manual (Scientific Instrument Services, Inc. Ringoes, NJ 08551, <<http://simion.com/>>, January 2008).
- [10]: D. Rodriguez, A. Méry, G. Ban, J. Brégeault, G. Darius, D. Durand, X. Fléhard, M. Herbane, M. Labalme, E. Liénard et al, D. Nucl. Instrum. Meth. in Phys. Res. A **565**, 876 (2006).
- [11]: X. Fléhard, Ph. Velten, E. Liénard et al., J. Phys. G: Nucl. Part. Phys **38**, 055101(2011).
- [12]: *Numerical recipes in C*, Second Edition, Cambridge University press, 1992.
- [13]: L. A. Viehland and E. A. Mason, Atomic and nuclear data tables **60**, 37 (1995).
- [14]: X. Fabian, F. Mauger, G. Quéméner, Ph. Velten, G. Ban, C. Couratin, P. Delahaye, D. Durand, B. Fabre, P. Finlay et al, Proceedings of the 6th International Conference on Trapped Charged Particles and Fundamental Physics (TCP 2014), Takamatsu, Japan, 1-5 December 2014, Hyp. Int. **235**, 87 (2015).

- [15]: “Analytical model of an ion cloud cooled by collisions in a Paul trap”, P. Delahaye, submitted to this journal.
- [16]: F. G. Major and H. G. Dehmelt, Phys. Rev. **170**, 91 (1968).
- [17]: X. Fléchar, G. Ban, D. Durand, E. Liénard, F. Mauger, A. Méry, O. Naviliat-Cuncic, D. Rodriguez, and P. Velten, Hyperfine Interact. **199**, 21 (2011).
- [18]: T. Kim, *Buffer gas cooling of ions in an RF ion guide: a study of the cooling process and cooled beam properties*, Ph.D. Thesis, McGill University, Montreal, 1997.
- [19]: E. Liénard, G. Ban, C. Couratin, P. Delahaye, D. Durand, et al., 6th International Conference on Trapped Charged Particles and Fundamental Physics (TCP 2014), Dec 2014, Takamatsu, Japan, Hyp. Int., **236**, 1 (2015).
- [20]: P. Delahaye et al, Hyp. Int., to appear in the proceedings of the Trapped Charged Particles 2018 conference.
- [21]: G. Neyens et al., Phys. Rev. Lett. **94**, 022501 (2005).
- [22]: M. Kowalska et al., Phys. Rev. C **77**, 034307 (2008).
- [23]: M. Schwarz et al, Rev. Sci. Instrum. **83**, 083115 (2012).
- [24]: S. Schwarz et al, Nucl. Instrum. Meth. B **204**,474 (2003).
- [25]: J.M. Cornejo, P. Escobedo, D. Rodríguez, Hyperfine Interact **227**,223(2014).
- [26]: J.M. Cornejo et al, submitted to Rev. Scient. Instrum.